



Cite this: *Chem. Commun.*, 2019, 55, 15125

Received 7th November 2019,
Accepted 19th November 2019

DOI: 10.1039/c9cc08679j

rsc.li/chemcomm

Fused twin-acridine scaffolds as electron donors for thermally activated delayed fluorescence emitters: controllable TADF behavior by methyl substitution†

Danyang Chai,^a Yang Zou,^{ib}*^a Yepeng Xiang,^b Xuan Zeng,^b Zhanxiang Chen,^b Shaolong Gong^{ib}^b and Chuluo Yang^{ib}*^{ab}

Fused twin-acridine scaffolds of TMQAC and MeTMQAC were designed as novel donors to construct new organic emitters. TMQAC-based emitters were TADF active, while the TADF character was turned off in MeTMQAC-based emitters by the extra methyl group. The TMQAC-based emitters exhibited high OLED performances, with external quantum efficiencies (EQEs) of up to 20.7%.

Exploring emitting materials with excellent device performance and low cost is currently of concern for the development of organic light emitting diodes (OLEDs). Among all the emitters, cost-effective purely organic thermally activated delayed fluorescence (TADF) emitters are recognized to have great potential owing to their triplet harvesting capability in devices which can realize a theoretical 100% internal quantum yield like noble metal-based phosphorescent emitters through a reverse intersystem crossing (RISC) process.¹ The key to enabling the TADF character for an emitter is to minimize the singlet–triplet splitting energy (ΔE_{ST}) between the molecular lowest singlet (S1) and the triplet state (T1).² According to the quantum theory, the ideal molecular design for TADF emitters is to realize a spatial separation between the highest occupied molecular orbital (HOMO) and lowest unoccupied molecular orbital (LUMO) distributions. In a typical donor–acceptor (D–A) type molecule, the HOMO and LUMO generally locate at the electron donor and acceptor, respectively. Based on this constitution, numerous efficient TADF emitters bearing a D–A architecture with sterically hindered bridges have been developed.³

So far, a vast number of acceptors with an electron-withdrawing nature have been intensively investigated for constructing TADF emitters.⁴ In contrast, the number of donor moieties used for TADF emitters is far less than that of acceptors.⁵ In this context, new design strategies for donors used for TADF emitters are highly demanded.

Among all the arylamine type electron donor moieties, 9,9-dimethyl-9,10-dihydroacridine (DMAC) has been the most widely and intensively investigated. TADF emitters based on DMAC usually exhibit small ΔE_{ST} s, high PLQYs, and good device performances.⁶ TADF emitters based on DMAC derivatives bearing a rigid spiral skeleton have been demonstrated to be excellent emitters for OLEDs.⁷ Aiming to construct efficient TADF emitters, in this study we designed a new electron donor by combining two DMAC moieties together, namely 12,12,14,14-tetramethyl-5,7,12,14-tetrahydro-quinolino[3,2-*b*]acridine (TMQAC), in which two nitrogen atoms located at the *meta* position to each other to regulate its electron donating ability, and the two DMAC units shared one central benzene ring to form a rigid ladder-type coplanar framework. When the TMQAC donor is equipped with two acceptors *via* C–N connection, the resulting emitter bearing a double D–A structure meets the demand for TADF molecules. First, the twisted D–A structure can endow the molecule with small ΔE_{ST} that enabled TADF. Second, it is known that connecting multiple D–A emitter moieties together in a single molecule may enhance the absorption and photoluminescence quantum yield (PLQY) of the emitters.⁸ Third, high molecular rigidity is crucial for boosting the PLQY as it can minimize the non-radiative transition process in the molecular excited state. For TMQAC-based emitters, two chromophore counterparts are locked up in a fused fashion; thus high molecular rigidity can be guaranteed. As expected, two TMQAC-based TADF emitters featuring a twin D–A structure with diphenyl sulphone (DPS) and triazine (TRZ) as acceptors exhibited an obvious TADF character and a high PLQY, and the resulting OLED devices achieved maximum quantum efficiencies (EQEs) of up to 20.7%. For comparison, another similar donor to TMQAC, namely MeTMQAC, in which an extra methyl group was attached on the central benzene ring, was designed and used to construct

^a Shenzhen Key Laboratory of Polymer Science and Technology, College of Materials Science and Engineering, Shenzhen University, Shenzhen 518060, People's Republic of China. E-mail: yangzou@szu.edu.cn, clyang@szu.edu.cn

^b Hubei Key Lab on Organic and Polymeric Optoelectronic Materials, Department of Chemistry, Wuhan University, Wuhan, 430072, People's Republic of China. E-mail: clyang@whu.edu.cn

† Electronic supplementary information (ESI) available: Experimental section, NMR spectra, TGA and electrochemical CV curves and temperature-dependent transient fluorescence spectra and OLED device data for TADF materials. CCDC 1961049–1961051. For ESI and crystallographic data in CIF or other electronic format see DOI: 10.1039/c9cc08679j



Scheme 1 Molecular structures of the emitters.

two compounds, namely DPS-MeTMQAC and TRZ-MeTMQAC. Unexpectedly, the methyl substitution remarkably affects the molecular geometry, and thus disables the TADF.

The molecular structures of TMQAC- and MeTMQAC-based emitters are depicted in Scheme 1, and their synthetic routes are shown in Schemes S1–S4 (see the ESI†). After treating methyl dicarboxylate with methyllithium, the obtained crude diol was directly reacted with a catalytic amount of boron trifluoride to obtain TMQAC *via* the intramolecular Friedel–Crafts cyclization process. MeTMQAC was synthesized in a similar way, except for using the corresponding ethylene as the ring closing substrate.⁹ After that, four emitters with a twin D–A structure were successively prepared through double Buchwald–Hartwig C–N coupling reactions between the corresponding donors and arylbromides. All the intermediates and the final products were obtained in good yields, and they are fully identified by ¹H and ¹³C nuclear magnetic resonance (NMR) spectroscopy as well as high-resolution electrospray ionization mass spectrometry (HR-ESI-MS), which are in good agreement with the theoretical results (Fig. S1–S12, ESI†). All four emitters exhibited excellent thermal stability with high decomposition temperatures (T_d , corresponding to 5% weight loss) over 400 °C as investigated by thermogravimetric analysis (Fig. S13, ESI†), which allowed them to be further refined by vacuum sublimation for device characterization.

Crystals of TRZ-TMQAC, DPS-TMQAC and DPS-MeTMQAC suitable for crystallography were grown by slowly evaporating their dichloromethane solutions. As shown in Fig. 1a, the donor moiety in TRZ-TMQAC adopted a nearly planar conformation, with one DMAC ring being quasi-equatorial, but the other one being quasi-axial.¹⁰ The two triazine acceptor moieties in TRZ-TMQAC were almost parallel to each other with a close distance of 4.1 Å, and they are highly twisted to the donor with dihedral angles of 77° and 87°. A similar molecular conformation was found in DPS-TMQAC as well (Fig. 1b). Unexpectedly, MeTMQAC-based emitters presented an entirely different

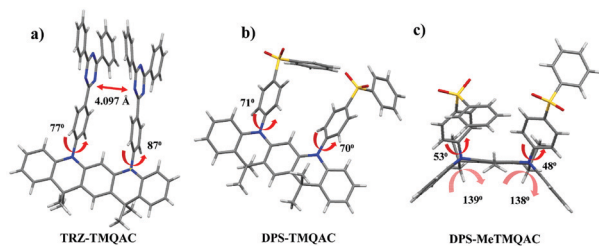


Fig. 1 X-ray crystal structures of (a) TRZ-TMQAC (CCDC: 1961049), (b) DPS-TMQAC (CCDC: 1961050) and (c) DPS-MeTMQAC (CCDC: 1961051).†

geometry from TMQAC-based emitters (Fig. 1c). The donor moiety in DPS-MeTMQAC was greatly distorted into a twist-boat conformation with large dihedral angles of 139° and 138°, while the acceptor moieties of DPS were less twisted to the donor with dihedral angles of 53° and 48° compared with TMQAC-based emitters.

The distinct single crystal X-ray structures of these emitters were in good agreement with their optimal molecular structures. As shown in Fig. 2, according to the optimized geometry obtained by density functional theory (DFT) and time dependent density functional theory (TD-DFT) with the B3LYP hybrid functional, the donor of TMQAC showed a nearly coplanar conformation, and large dihedral angles of 86° and 86° between the TRZ acceptors and the TMQAC donor were observed. In contrast, the MeTMQAC donor part was greatly distorted into a twist-boat conformation due to the steric hindrance of the extra methyl group, and thus resulted in much smaller twisting angles of 46°/50° between the TRZ acceptors and the TMQAC donor. Similar results were obtained when DPS was selected as an acceptor (Fig. S14, ESI†). All the calculated data are summarized in Table S1 (ESI†). Noticeably, the difference in molecular geometry led to distinct molecular energy levels, orbital distributions and ΔE_{ST} s. A very good HOMO–LUMO separation was predicted for TRZ-TMQAC, resulting in an ultra-small ΔE_{ST} of 0.01 eV that could facilitate RISC. However, for TRZ-MeTMQAC, the remarkably overlapped HOMO–LUMO levels on the bridging benzene ring between the donor and acceptor led to a large ΔE_{ST} of 0.33 eV. Similar calculated results were acquired for the two emitters with the DPS acceptor as well (Fig. S14 and Table S1, ESI†).

The distinct molecular structures of TMQAC- and MeTMQAC-based emitters revealed by simulation and X-ray crystallography implied their remarkably different properties. As investigated by cyclic voltammetry (CV) experiments (Fig. S16, ESI†), TMQAC-based emitters exhibited much shallower HOMO levels (−5.11 eV for TRZ-TMQAC and −5.23 eV for DPS-TMQAC) than their analogues with the MeTMQAC donor (−5.53 eV for TRZ-MeTMQAC and −5.64 eV for DPS-MeTMQAC). According to the UV-vis spectroscopy (Fig. 3a), TRZ-TMQAC showed a strong absorption band at 300–350 nm corresponding to localized π – π^* and n – π^* transitions, along with a broad characteristic band at 350–450 nm assigned to intramolecular charge transfer (ICT).

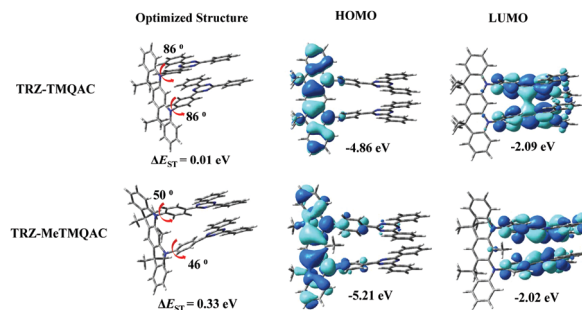


Fig. 2 The optimal geometric structures and molecular frontier orbital distributions of TRZ-TMQAC and TRZ-MeTMQAC obtained by theoretical calculations.

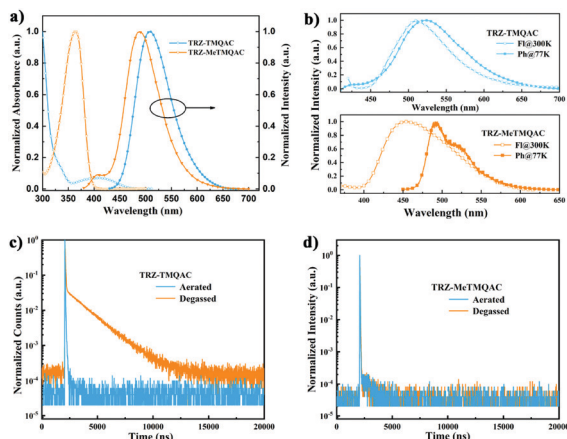


Fig. 3 Optical properties of TRZ-TMQAC and TRZ-MeTMQAC: (a) UV-vis and fluorescence spectra in toluene solution, (b) fluorescence at 300 K and phosphorescence at 77 K of 10 wt% emitters doped into a DPEPO host, and (c and d) the transient photoluminescence decay curves of the emitters in toluene (10^{-5} M) under degassed and aerated conditions.

On the other hand, for TRZ-MeTMQAC, no clear ICT absorption band was observed,¹¹ and only a localized $\pi-\pi^*$ and $n-\pi^*$ transition peak at 364 nm was found, which was typical for a D-A emitter with a sterically hindered donor.¹² In the fluorescence spectrum (Fig. 3a), TRZ-TMQAC showed a green emission peak at 510 nm in toluene with clear ICT character proved by solvatochromism experiments (Fig. S16, ESI[†]). In contrast, because of the highly distorted donor arising from methyl substitution, TRZ-MeTMQAC exhibited a blue-shifted spectrum with an emission peak at 488 nm in toluene, along with a weak emission at 400 nm that originated from the local emission of the donor.¹² According to the phosphorescence spectra of their films in bis[2-(diphenylphosphino)phenyl]ether oxide (DPEPO) recorded at 77 K (Fig. 3b), the triplet energy can be obtained (Table 1). Accordingly, TMQAC-based emitters exhibited ultra-small ΔE_{ST} s less than 0.10 eV, while MeTMQAC-based emitters exhibited large ΔE_{ST} s more than 0.40 eV.

To further illustrate the impact of methyl substitution on photophysical properties, the transient photoluminescence decay curves of the emitters in toluene solution were measured. As shown in Fig. 3c and Fig. S18b (ESI[†]), both TMQAC-based emitters exhibited clear double-exponential decay curves under an argon atmosphere, accompanied by fitting prompt and delayed fluorescence (DF) lifetimes of 37.68 ns/1.62 μ s for TRZ-TMQAC and 24.89 ns/1.55 μ s for DPS-TMQAC. In addition,

their DF components were almost quenched by oxygen under aerated conditions, which obviously proved their TADF character. Similar decay curves with typical double-exponential character were found for their films in DPEPO (Fig. S19, ESI[†]), with high PLQYs of 73% and 74% for TRZ-TMQAC and DPS-TMQAC, respectively. In sharp contrast, no long lifetime on a micro-second scale could be observed for either TRZ-MeTMQAC or DPS-MeTMQAC even under degassed conditions (Fig. 3d and Fig. S18c, ESI[†]), suggesting that the RISC process was disabled, which also led to their low PLQYs in the DPEPO films (Table 1).

The distinct photoluminescent properties of these emitters could reflect on their device performances. To validate this, OLEDs with an ITO/HAT-CN (5 nm)/TPAC (30 nm)/mCP (10 nm)/EML (20 nm)/DPEPO (10 nm)/TmPyPB (30 nm)/Liq (1.5 nm)/Al (100 nm) device configuration were fabricated, where ITO and Al acted as an anode and a cathode, respectively; 1,4,5,8,9,11-hexaazatriphenylene-hexacarbonitrile (HAT-CN) and lithium 8-quinolinolate (Liq) were used as hole and electron-injection layers, respectively; 1,1-bis[(di-4-tolylamino)phenyl]cyclohexane (TAPC) and 1,3,5-tri(*m*-pyrid-3-ylphenyl)benzene (TmPyPb) were used as hole- and electron transport materials, respectively; and 1,3-bis(*N*-carbazoyl)benzene (mCP) was used as an electron/exciton blocking layer. DPEPO was employed as the host owing to its high energy level of 4.1 eV, and all four emitters were doped into the DPEPO host with a doping concentration of 10 wt% to act as the emitting layer. The devices results are summarized in Table S2 (ESI[†]).

As shown in Fig. 4c, both TMQAC-based emitters showed identical electroluminescence (EL) spectra to their photoluminescence (PL) spectra. TRZ-TMQAC displayed green emission with Commission International de l'Eclairage (CIE) coordinates of (0.30, 0.56), while DPS-TMQAC showed sky-blue emission with CIE coordinates of (0.19, 0.33). More importantly, both TMQAC-based devices presented significantly superior device performance to the MeTMQAC-based ones. For example, TRZ-TMQAC-based device displayed a maximum external quantum efficiency (EQE) of 20.7%, a maximum current efficiency (CE_{max}) of 66.1 cd A⁻¹, and a maximum power efficiency (PE_{max}) of 51.9 lm W⁻¹. However, TRZ-MeTMQAC under the same device configuration exhibited a much lower EQE_{max} of 5.5%, CE_{max} of 8.3% and PE_{max} of 6.5%. The same trend was found for DPS-TMQAC- and DPS-MeTMQAC-based devices (EQE_{max} of 14.3% vs. 1.2%, Fig. S20, ESI[†]). The superior device performance with an EQE_{max} of over 20% further proved the TADF character for TMQAC-based emitters. In contrast, MeTMQAC-based emitters are only traditional fluorescent emitters.

Table 1 The physical properties and kinetic parameters of the compounds

Compound	λ_{abs}^a [nm]	λ_{em}^b [nm]	HOMO/LUMO ^c [eV]	$S_1/T_1/\Delta E_{ST}^d$	τ_{PF}/τ_{DF}^e [ns]/[μ s]	DF ratio ^e (%)	Φ_{PL}^f
TRZ-TMQAC	296, 406	508/522	-5.11/-2.48	2.74/2.72/0.02	39/1.01	78	73
TRZ-MeTMQAC	364	487/454	-5.53/-2.44	2.97/2.93/0.44	—	—	43
DPS-TMQAC	295, 320, 372	473/471	-5.23/-2.33	3.07/2.63/0.04	30/3.09	90	74
DPS-MeTMQAC	310	453/418	-5.64/-2.20	3.49/3.06/0.43	—	—	33

^a Measured in toluene solutions (10^{-5} M) at 298 K. ^b Measured in toluene solutions/in the DPEPO films. ^c The HOMOs were calculated from CV; LUMO = HOMO + E_g^{opt} . ^d Calculated from the onset wavelengths of the fluorescence (298 K) and phosphorescence (77 K) spectra of both emitters in the DPEPO host. ^e The fitting lifetimes of the prompt and DF components and the DF ratios of both emitters in toluene solution. ^f PLQYs of 10 wt% both emitters doped into the DPEPO host.

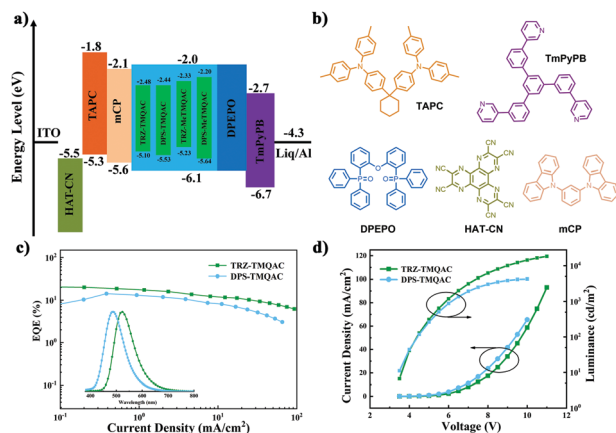


Fig. 4 (a) The energy level diagrams and (b) chemical structures of the materials used in the devices. (c) External quantum efficiency–current density curves. Inset: The EL spectra at 10 V. (d) Luminescence and current density versus voltage characteristics.

In summary, two fused twin-acridine donors TMQAC and MeTMQAC were designed. Four emitters with a twin D–A structure were further synthesized by connecting donors with TRZ or DPS acceptors. Clearly, the TMQAC- and MeTMQAC-based emitters presented remarkably different molecular conformations as proved by X-ray crystallography and theoretical simulation. Their distinct molecular conformations had profound consequences on their photophysical properties. TRZ-TMQAC and DPS-TMQAC are TADF active, while MeTMQAC-based emitters with an extra methyl group are TADF inactive. Thanks to the TADF character of the TMQAC-based emitters, the resulting OLEDs exhibited high performances, with EQE_{max} values of 20.7% and 14.3% for TRZ-TMQAC and DPS-TMQAC based devices, respectively. This work reveals that the fused twin-acridine is a promising donor to construct efficient TADF emitters.

We gratefully acknowledge financial support from the National Natural Science Foundation of China (Grant No. 51703131 and 91833304), the Shenzhen Peacock Plan (KQTD20170330110107046), the Shenzhen Technology and Innovation Commission (JCYJ20180507182244027) and the Natural Science Foundation of SZU (Grant No. 2018001). We thank the Instrumental Analysis Center of Shenzhen University for analytical support.

Conflicts of interest

There are no conflicts to declare.

References

- H. Uoyama, K. Goushi, K. Shizu, H. Nomura and C. Adachi, *Nature*, 2012, **492**, 234.
- (a) Q. Zhang, J. Li, K. Shizu, S. Huang, S. Hirata, H. Miyazaki and C. Adachi, *J. Am. Chem. Soc.*, 2012, **134**, 14706–14709; (b) S. Hirata, Y. Sakai, K. Masui, H. Tanaka, S. Y. Lee, H. Nomura, N. Nakamura, M. Yasumatsu, H. Nakanotani, Q. Zhang, K. Shizu, H. Miyazaki and C. Adachi, *Nat. Mater.*, 2015, **14**, 330.
- (a) Y. Tao, K. Yuan, T. Chen, P. Xu, H. Li, R. Chen, C. Zheng, L. Zhang and W. Huang, *Adv. Mater.*, 2014, **26**, 7931; (b) M. Y. Wong and E. Zysman-Colman, *Adv. Mater.*, 2017, **29**, 1605444; (c) Z. Yang, Z. Mao, Z. Xie, Y. Zhang, S. Liu, J. Zhao, J. Xu, Z. Chi and M. P. Aldred, *Chem. Soc. Rev.*, 2017, **46**, 915.
- (a) I. S. Park, S. Y. Lee, C. Adachi and T. Yasuda, *Adv. Funct. Mater.*, 2016, **26**, 1813; (b) J. Zhang, D. Ding, Y. Wei, F. Han, H. Xu and W. Huang, *Adv. Mater.*, 2016, **28**, 479; (c) W. Zeng, H. Y. Lai, W. K. Lee, M. Jiao, Y. J. Shiu, C. Zhong, S. Gong, T. Zhou, G. Xie, M. Sarma, K. T. Wong, C. C. Wu and C. Yang, *Adv. Mater.*, 2018, **30**, 1704961.
- (a) J. W. Sun, J. Y. Baek, K.-H. Kim, J.-S. Huh, S.-K. Kwon, Y.-H. Kim and J.-J. Kim, *J. Mater. Chem. C*, 2017, **5**, 1027; (b) S. J. Woo, Y. Kim, Y. H. Kim, S. K. Kwon and J. J. Kim, *J. Mater. Chem. C*, 2019, **7**, 4191.
- (a) Y. Wada, K. Shizu, S. Kubo, K. Suzuki, H. Tanaka, C. Adachi and H. Kaji, *Appl. Phys. Lett.*, 2015, **107**, 183303; (b) L. Yu, Z. Wu, G. Xie, W. Zeng, D. Ma and C. Yang, *Chem. Sci.*, 2018, **9**, 1385; (c) W. Li, X. Cai, B. Li, L. Gan, Y. He, K. Liu, D. Chen, Y. C. Wu and S. Su, *Angew. Chem., Int. Ed.*, 2019, **58**, 582.
- (a) M. Liu, R. Komatsu, X. Y. Cai, K. Hotta, S. Sato, K. K. Liu, D. C. Chen, Y. Kato, H. Sasabe, S. Ohisa, Y. Suzuri, D. Yokoyama, S. Su and J. Kido, *Chem. Mater.*, 2017, **29**, 8630; (b) X. Zeng, K.-C. Pan, W.-K. Lee, S. Gong, F. Ni, X. Xiao, W. Zeng, Y. Xiang, L. Zhan, Y. Zhang, C.-C. Wu and C. Yang, *J. Mater. Chem. C*, 2019, **7**, 10851.
- (a) M. Kim, S. K. Jeon, S.-H. Hwang, S.-S. Lee, E. Yu and J. Y. Lee, *Chem. Commun.*, 2016, **52**, 339; (b) H.-J. Park, S. H. Han and J. Y. Lee, *J. Mater. Chem. C*, 2017, **5**, 12143; (c) D. Wei, F. Ni, Z. Wu, Z. Zhu, Y. Zou, K. Zheng, Z. Chen, D. Ma and C. Yang, *J. Mater. Chem. C*, 2018, **6**, 11615.
- L. Skórka, J.-M. Mouesca, J. B. Gosk, R. Puźniak, J. Pécaut, V. Maurel and I. Kulszewicz-Bajer, *J. Mater. Chem. C*, 2017, **5**, 6563.
- K. Wang, C. Zheng, W. Liu, K. Liang, Y. Shi, S. L. Tao, C. S. Lee, X. M. Ou and X. Zhang, *Adv. Mater.*, 2017, **29**, 1701476.
- Y. Geng, A. D'Aleo, K. Inada, L. S. Cui, J. U. Kim, H. Nakanotani and C. Adachi, *Angew. Chem., Int. Ed.*, 2017, **56**, 16536.
- (a) Q. Zhang, S. Sun, W. J. Chung, S. J. Yoon, Y. Wang, R. Guo, S. Ye, J. Y. Lee and L. Wang, *J. Mater. Chem. C*, 2019, **7**, 12248; (b) S. G. Yoo, W. Song and J. Y. Lee, *Dyes Pigment.*, 2016, **128**, 201.